Available online at www.sciencedirect.com
ScienceDirect
International Journal of Pharmaceutics 355 (2008) 238–248
INTERNATIONAL JOURNAL OF PHARMACEUTICS
www.elsevier.com/locate/ijpharm

Cytokine and IDO metabolite changes effected by calcium pterin during inhibition of MDA-MB-231 xenograph tumors in nude mice

Phillip Moheno [a,*], Wolfgang Pfleiderer [b], Antonio G. DiPasquale [c], Arnold L. Rheingold [c], Dietmar Fuchs [d]

[a] *SanRx Pharmaceuticals, Inc., 603 Colima Street, La Jolla, CA 92037, USA*
[b] *Fachbereich Chemie, University of Konstanz, Universitaetsstrasse 10, D-78457 Konstanz, Germany*
[c] *Small Molecule X-ray Facility, Department of Chemistry and Biochemistry, University of California, San Diego, 9500 Gilman Drive, La Jolla, CA 92093, USA*
[d] *Division of Biological Chemistry, Biocentre, Innsbruck Medical University, Fritz Pregl Strasse 3, A-6020 Innsbruck, Austria*

Received 24 July 2007; received in revised form 15 December 2007; accepted 17 December 2007
Available online 24 December 2007

Abstract

In vivo studies of the effectiveness of various forms of calcium pterin reveal significant antitumor activity associated with (1:4, mol/mol) calcium pterin (CaPterin), (1:2, mol/mol) calcium pterin, dipterinyl calcium pentahydrate (DCP), as well as unexpectedly for a calcium chloride dihydrate solution in nude mice with MDA-MB-231 xenographs. Stepwise regression analysis of nine plasma cytokine and indoleamine 2,3-dioxygenase (IDO) metabolite levels identified four effects correlated to (1:4, mol/mol) calcium pterin administration: (1) decreased IL-6, (2) increased IL-10, (3) decreased IFN-γ, and (4) increased kynurenine. *Conclusion*: (1:4, mol/mol) CaPterin exerts significant (by Spearman rank order correlation) dose–response antitumor activity in nude mice with MDA-MB-231 xenographs, and sustains both inflammatory and anti-inflammatory changes in the levels of certain plasma factors.

Keywords: Oral antitumor compounds; Immunomodulatory and cytokine effects

1. Introduction

Since the discovery and elucidation of the antitumor properties of calcium pterin (Moheno, 2004; Winkler et al., 2006), it has become important to identify stable, effective calcium pterin complex forms, as well as to further specify their immunomechanism(s) of action. The current study reports on advances in both these areas, and the synthesis and characterization of a promising new cancer therapeutic, dipterinyl calcium pentahydrate (DCP).

A suspension of calcium pterin in the molar ratio of 1:4 calcium to pterin (2-amino-4(3*H*)-pteridinone) known as CaPterin was found to possess significant antitumor efficacy against MDA-MB-231 human breast xenographs in nude mice, as well as highly significant activity against spontaneous mammary gland tumors in C3H/HeN−MTV+ mice, based upon National Cancer Institute standards (Moheno, 2004). An immunomodulatory mode of action for CaPterin was deduced by comparing the antitumor efficacy of CaPterin in four different mouse/tumor systems, i.e., the two cited above, as well as in Balb/c mice with EMT6 xenographs and SCID mice with MDA-MB-231 xenographs. The further specification of the immunological effects of CaPterin in nude mice with MDA-MB-231 xenographs is herein described. In the present study, the nude mouse tumor system was chosen because of the human origin of the tumor xenographs and the uniformity of the tumors produced. In an

* Corresponding author. Tel.: +1 858 344 9778; fax: +1 858 454 6134.
E-mail addresses: phil.moheno@sanrx.com (P. Moheno), wolfgang.pfleiderer@uni-konstanz.de (W. Pfleiderer), adipasqu@chem.ucsd.edu (A.G. DiPasquale), arnrhein@chem.ucsd.edu (A.L. Rheingold), dietmar.fuchs@i-med.ac.at (D. Fuchs).

0378-5173/$ – see front matter © 2007 Elsevier B.V. All rights reserved.
doi:10.1016/j.ijpharm.2007.12.021

effort to expand the characterization of the active forms of calcium pterin, antitumor data are also presented for (1:2, mol/mol) calcium pterin, as well as for dipterinyl calcium pentahydrate at two dosages. In addition, comparative antitumor efficacy results are given for pterin and a calcium chloride dihydrate solution, the latter at a Ca^{2+} concentration equivalent to that contained in the (1:4, mol/mol) calcium pterin suspension (CaPterin) administered at 21 mg/(kg day).

Because *in vitro* studies suggest that the antitumoral effects of CaPterin involve the immunomodulatory actions of NK cell activation and indoleamine 2,3-dioxygenase (IDO) inhibition (Moheno et al., 2005; Winkler et al., 2006), the investigators herein analyse the *in vivo* immunological effects evoked by CaPterin based upon the measurement of ten plasma components: IL-1b, IL-2, IL-4, IL-6, IL-10, IL-12, IFN-γ, TNF-α, tryptophan (Trp), and kynurenine (Kyn). Kynurenine/tryptophan (Kyn/Trp) ratios were calculated as a measure of IDO activity (Wirleitner et al., 2003), previously shown to be inhibited *in vitro* by CaPterin in human PBMCs (peripheral blood mononuclear cells) (Winkler et al., 2006).

2. Materials and methods

2.1. Test substances

2.1.1. (1:4, mol/mol) Calcium pterin suspension (1 mg/ml)

Suspension A is prepared by mixing 24 mg pterin (Schircks Laboratories, Jona, Switzerland) into 30 ml distilled H_2O. Suspension B is prepared by first dissolving 8 mg $CaCl_2{\cdot}2H_2O$ into 10 ml distilled H_2O, then mixing in 8 mg pterin. Suspension B is then mixed with suspension A yielding 40 ml of 1 mg/ml (1:4, mol/mol) calcium pterin suspension.

2.1.2. Pterin suspension (1 mg/ml)

Prepared by mixing 40 mg pterin in 40 ml distilled H_2O.

2.1.3. (1:2, mol/mol) Calcium pterin suspension (1.2 mg/ml)

Suspension A is prepared by mixing 16 mg pterin into 30 ml distilled H_2O. Suspension B is prepared by first dissolving 16 mg $CaCl_2{\cdot}2H_2O$ into 10 ml distilled H_2O, then mixing in 16 mg pterin. Suspension B is then mixed with suspension A yielding 40 ml of 1.2 mg/ml (1:2, mol/mol) calcium pterin suspension.

2.1.4. Dipterinyl calcium pentahydrate synthesis

Pure pterin (81.7 mg, 0.5 mmol) was dissolved in H_2O (50 ml) and 0.1N NaOH (6 ml) and $CaCl_2{\cdot}2H_2O$ (36.7 mg, 0.25 mmol) was added to the clear solution with stirring (pH 10.93). A yellowish precipitate was formed within a few minutes. Stirring was continued for 1 day and then the precipitate collected and dried in a vacuum desiccator to give 75 mg. The elemental analysis is consistent with $(C_6H_4N_5O)_2Ca{\cdot}5H_2O$ (MW 454.4). Calc.: C 31.74, H 4.00 and N 30.85; found: C 31.22, H 3.97 and N 29.83.

Comparison of the extinctions of the UV spectra of pterin and $(C_6H_4N_5O)_2Ca{\cdot}5H_2O$ taken at pH 13 give the following: Pterin: 223 nm (8700), 250 nm (21,380) and 357 nm (8510); $(C_6H_4N_5O)_2Ca{\cdot}5H_2O$: 223 nm (14,450), 250 nm (39,810) and 357 nm (13,490).

2.1.5. Dipterinyl calcium pentahydrate suspensions

A 1.1 mg/ml suspension was prepared by mixing 44 mg dipterinyl calcium pentahydrate in 40 ml distilled H_2O. A 3.3 mg/ml suspension was prepared by mixing 132 mg dipterinyl calcium pentahydrate in 40 ml distilled H_2O.

2.1.6. $CaCl_2{\cdot}2H_2O$ solution (0.2 mg/ml)

Prepared by dissolving 8 mg $CaCl_2{\cdot}2H_2O$ into 40 ml distilled H_2O.

2.2. Fourier transformed infrared spectrophotometry

Infrared spectra (Fig. 1) were determined using a Nicolet Impact 400 QSE 335/045, by Quadrant Scientific, Inc. (San Diego, CA).

2.3. X-ray crystallographic analysis

2.3.1. Calcium pterin

Crystal plates were grown from (1:4, mol/mol) calcium pterin suspension after solubilization with mild aqueous NaOH. A yellow plate 0.08 mm × 0.08 mm × 0.03 mm in size was mounted on a cryoloop with paratone oil. Data were collected in a nitrogen gas stream at 100(2) K using phi and omega scans. Crystal-to-detector distance was 60 mm and exposure time was 20 s per frame using a scan width of 0.5°. Data collection was 99.4% complete to 25.00° in θ. A total of 7203 reflections were collected covering the indices, $-9 \le h \le 8$, $-20 \le k \le 19$, $-9 \le l \le 11$. 1843 Reflections were found to be symmetry independent, with a R_{int} of 0.0932. Indexing and unit cell refinement indicated a primitive, monoclinic lattice. The space group was found to be $P2(1)/c$ (no. 14). The data were integrated using the Bruker SAINT software program and scaled using the SADABS software program. Solution by direct methods (SIR-97) produced a complete heavy-atom phasing model consistent with the proposed structure. All non-hydrogen atoms were refined anisotropically by full-matrix least-squares (SHELXL-97). All hydrogen atoms were placed using a riding model. Their positions were constrained relative to their parent atom using the appropriate HFIX command in SHELXL-97. The derived structure is given in Fig. 2A.

2.3.2. Dipterinyl calcium pentahydrate

Crystal plates were grown from DCP suspension after solubilization with mild aqueous NaOH. A yellow plate 0.12 mm × 0.10 mm × 0.05 mm in size was mounted on a cryoloop with paratone oil. Data were collected in a nitrogen gas stream at 100(2) K using phi and omega scans. Crystal-to-detector distance was 60 mm and exposure time was 20 s per frame using a scan width of 0.5°. Data collection was 99.6% complete to 25.00° in θ. A total of 6501 reflections were collected covering the indices, $-8 \le h \le 8$, $-19 \le k \le 19$, $-9 \le l \le 9$. 1682 reflections were found to be symmetry independent, with a R_{int} of 0.0561. Indexing and unit cell refinement

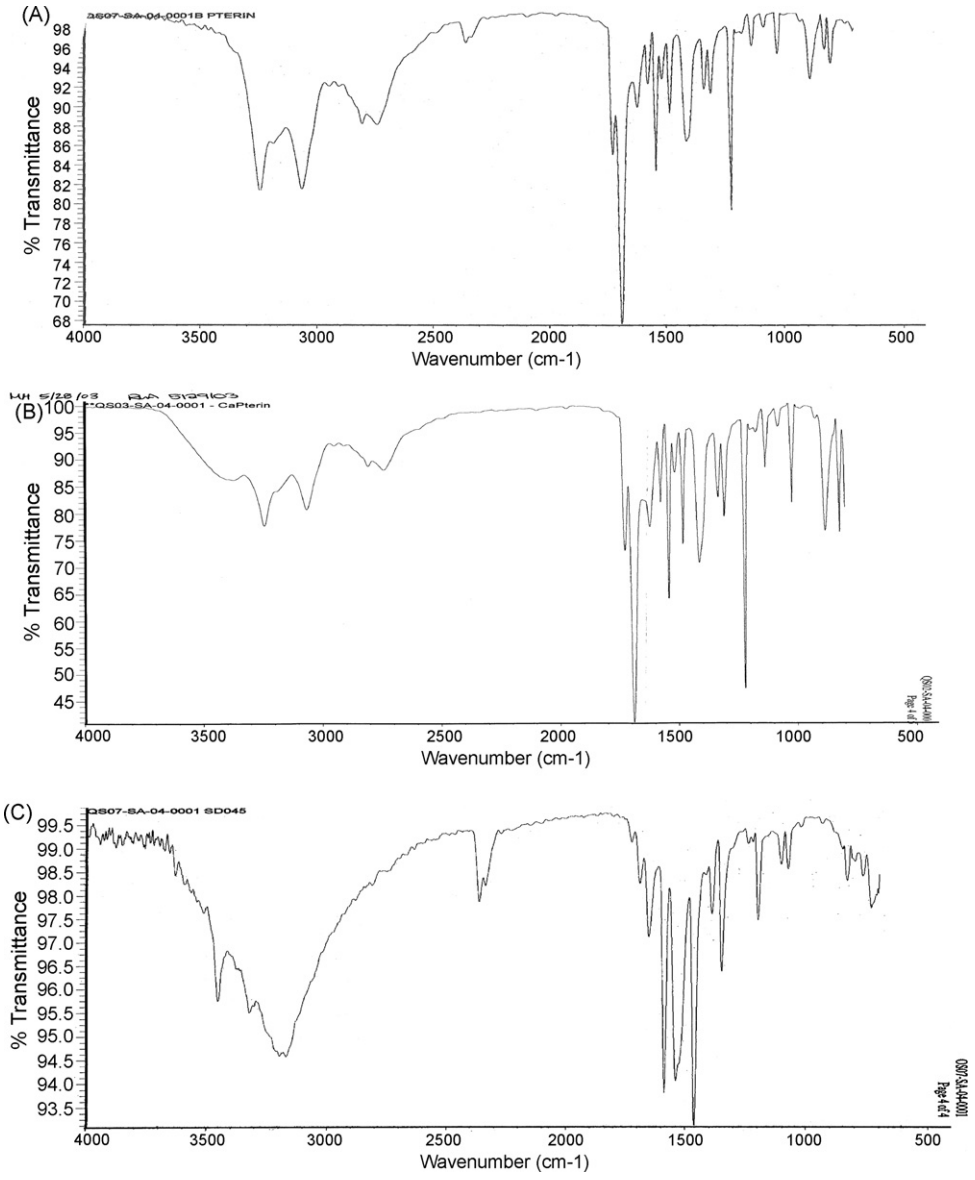

Fig. 1. Fourier transformed infrared spectra of (A) pterin, (B) (1:4, mol/mol) calcium pterin, and (C) dipterinyl calcium pentahydrate (DCP) (SD045).

indicated a primitive, monoclinic lattice. The space group was found to be *P*2(1)/*m* (no. 11). The data were integrated using the Bruker SAINT software program and scaled using the SADABS software program. Solution by direct methods (SIR-97) produced a complete heavy-atom phasing model consistent with the proposed structure. All non-hydrogen atoms were refined anisotropically by full-matrix least-squares (SHELXL-97). All hydrogen atoms were placed using a riding model. Their positions were constrained relative to their parent atom using the appropriate HFIX command in SHELXL-97. The derived structure for DCP is given in Fig. 2B.

2.4. In vivo testing

2.4.1. Protocol

2.4.1.1. First Experiment. The aims of the first experiment were to determine a dose–response curve for the (1:4, mol/mol) calcium pterin suspension, to compare the antitumor activity of this suspension to pterin alone (pterin control), and to test the effect of CaPterin mega-dosing at 100 mg/(kg day). Antitumor efficacy was evaluated in nude mice with MDA-MB-231 human tumor xenographs by Perry Scientific (San Diego, CA). In the first experiment, 23 athymic nude (nu/nu) female mice, ages 3–4 weeks, were purchased from Harlan Sprague Dawley, Inc. (Indianapolis, IN). 5×10^6 MDA-MB-231 cancer cells were injected subcutaneously into the right flank of each mouse. When tumors reached 3–5 mm in size, 20 mice were divided into four treatment/control groups of five mice each. The four treatment groups were: (1:4, mol/mol) calcium pterin (7 mg/(kg day)); pterin (21 mg/(kg day)); (1:4, mol/mol) calcium pterin (21 mg/(kg day)); and sterile water control. Two mice with outlying tumor sizes or non-tumor takes were excluded shortly after treatment began: one from the pterin group and one from the control group. Any tumor which did not persist for >14 days was considered to be outlying statistically and was therefore not included in the final metabolic analysis. Only one outlier per-

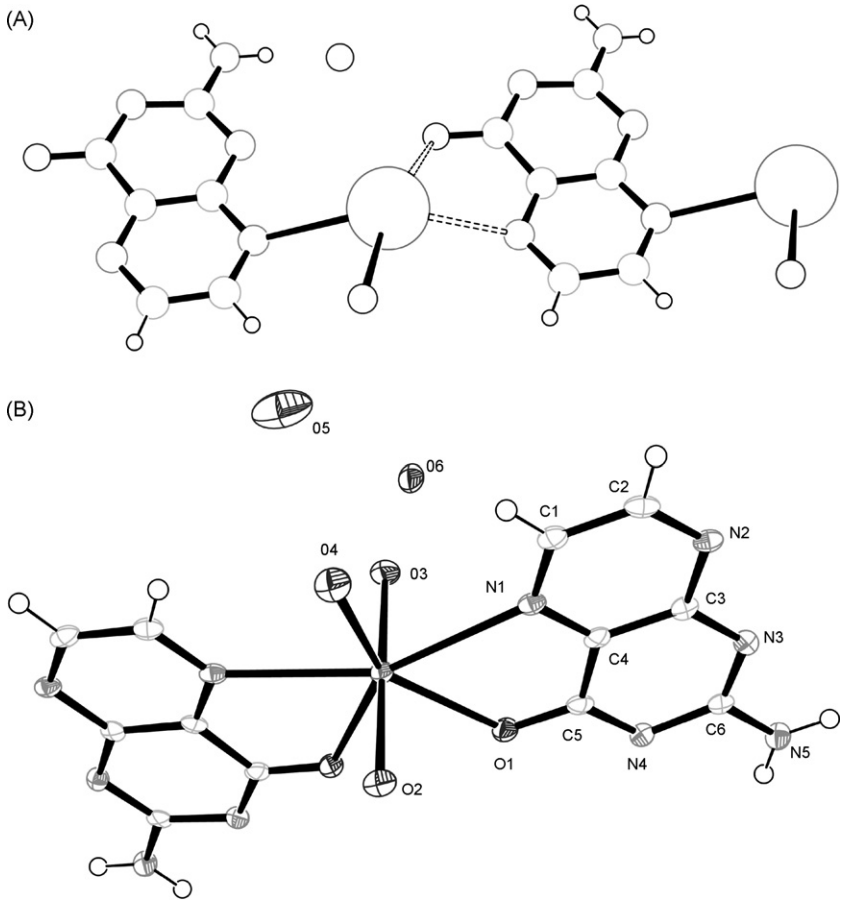

Fig. 2. X-ray crystallographic structure of (A) calcium pterin, and (B) dipterinyl calcium pentahydrate (DCP).

sisted >4 days, for 14 days. Also excluded from the metabolic analysis in the first experiment was one mouse from each of the four experimental groups mega-dosed by oral gavage with 100 mg/(kg day) CaPterin for up to 31 days to test for toxicity. All the other mice in the first experiment persisted ≥60 days without complications.

2.4.1.2. Second Experiment. The aims of the second experiment were three-fold: (1) to test the antitumor effect of the increased [Ca^{2+}] in the (1:2, mol/mol) calcium pterin suspension compared to the (1:4, mol/mol) calcium pterin suspension; (2) to evaluate the antitumor efficacy of DCP at two concentrations, 23 and 69 mg/(kg day); and (3) to evaluate the antitumor activity of the calcium pterin to calcium chloride alone ($CaCl_2$ control). In the second experiment, 29 athymic nude, also purchased from Harlan Sprague Dawley, Inc. (Indianapolis, IN), were each injected subcutaneously with 10×10^6 MDA-MB-231 cancer cells into the right flank. When tumors reached 3–5 mm in size, the mice were divided into five treatment groups of five each and a control group of four mice. The five treatment groups were: (1:4, mol/mol) calcium pterin (21 mg/(kg day)); (1:2, mol/mol) calcium pterin (25 mg/(kg day)); DCP (23 mg/(kg day)); DCP (69 mg/(kg day)); and calcium chloride dihydrate (4.2 mg/(kg day)). Four of these mice with outlying tumor sizes or non-tumor takes were excluded shortly after treatment began: one each from the (1:4, mol/mol) calcium pterin group, the (1:2, mol/mol) calcium pterin group, the DCP (69 mg/(kg day)) group, and one from the control group. All the other mice in the second experiment persisted ≥43 days without complications. Experimental groups were treated by oral gavage once daily with the indicated test suspensions or solutions.

The control mice in the first experiment were treated with sterile water while the control mice in the second experiment were untreated to evaluate the effect of mouse handling and gavaging upon tumor growth. Daily dosing was for 7 days per week. Animals were restrained but not anesthetized for oral dosing. Tumors were measured twice weekly with calipers and body weights taken twice weekly on the day of tumor measurements. Blood was collected from all animals via cardiac puncture at termination (after 70–98 days of treatment) and processed to EDTA plasma for analysis. Tumor size measurements for the control group in the second experiment on days 4 and 7 were missed due to a technical oversight.

2.4.2. Cell line propagation and inoculation

The MDA-MB-231 human breast tumor cell lines were supplied by SRI International (Menlo Park, CA) and propagated using standard *in vitro* cell expansion methods. Briefly, cells were grown in L-15 media from Gibco (Cat. no. 11415-064) supplemented with 2 mM L-glutamine and 10% fetal bovine serum (FBS). The cells were cultured in an incubator with 5% CO_2, 37.5 °C, and 80% humidity. Cells were harvested with 0.25%

Table 1
Blood was collected from the mice in the first experiment via cardiac puncture at sacrifice after Day 60 and processed to EDTA plasma for analysis

	Control ($N=3$) (sterile H_2O)	CaPterin ($N=3$) (7 mg/(kg day))	CaPterin ($N=4$) (21 mg/(kg day))
Day 60 relative tumor volumes	20.4 ± 3.4	24.0 ± 9.0	7.9 ± 1.3
IL-1b (pg/ml)	n.d.	5.2 ± 2.0	3.4 ± 0.2
IL-2 (pg/ml)	n.d.	n.d.	n.d.
IL-4 (pg/ml)	n.d.	n.d.	n.d.
IL-6 (pg/ml)	104.5 ± 10.9	114.7 ± 43.2	121.7 ± 78.1
IL10 (pg/ml)	n.d.	41.9 ± 22.7	50.8 ± 32.3
IL-12 (pg/ml)	n.d.	7.7 ± 4.4	243.8 ± 237.8
IFN-γ (pg/ml)	n.d.	4.7 ± 0.6	n.d.
TNF-α (pg/ml)	4.3 ± 0.5	9.8 ± 1.5	8.5 ± 1.6
Kynurenine (μM)	1.4 ± 0.2	1.2 ± 0.2	1.8 ± 0.3
Tryptophan (μM)	93.6 ± 3.1	87.9 ± 14.6	106.5 ± 7.8
Kyn/Trp (μM/mM)	14.4 ± 2.1	14.1 ± 0.2	17.5 ± 3.8

One mouse from each of the two CaPterin groups and the Control group, i.e., three mice, were excluded from this analysis because they were used to test the effects of mega-dosing after Day 60 of treatment. Also, one mouse from the CaPterin (7 mg/(kg day)) treatment group expired suddenly before cardiac puncture could be carried out. Plasma cytokine levels were determined by ELISA assay (n.d. = not detectable; <3.2 pg/ml). IDO Metabolite levels were determined by HPLC. All values are given as means ± S.E.M.

(w/v) trypsin–0.03% (w/v) EDTA solution. Cells were prepared for injection by standard methods to appropriate concentrations. Animals were temporarily restrained but not anesthetized for the inoculation of the tumor cells. Animals were subcutaneously injected with the tumor cells in a 100–200 μl volume.

2.4.3. Animal care

The animals were housed four to a cage in approved micro-isolator cages. Caging bedding and related items were autoclaved prior to use. No other species were housed in the same room(s) as the experimental animals. The rooms were well ventilated (greater than 10 air changes per hour) with 100% fresh air (no air recirculation). A 12-h light/12-h dark photoperiod was maintained, except when room lights were turned on during the dark cycle to accommodate study procedures. Room temperature was maintained between 16 and 22 °C. Animal room and cage cleaning was performed according to Perry Scientific SOP (standard operating procedure). Animals had *ad libitum* access to irradiated PicoLab Rodent Diet 20 mouse chow. Autoclaved and chlorinated, municipal tap water was available *ad libitum* to each animal via water bottles.

Treatment of the animals was in accordance with Perry Scientific SOP, which adhered to the regulations outlined in the USDA Animal Welfare Act (9 CFR [Code of Federal Regulations], parts 1–3) and the conditions specified in The Guide for Care and Use of Laboratory Animals (ILAR [Institute for Laboratory Animal Research] publication, 1996, National Academy Press). The protocol was approved by Perry Scientific's Institutional Animal Care and Use Committee prior to initiation of the study. The study conduct was in general compliance with the US FDA Good Laboratory Practice Regulations currently in effect (21 CFR, part 58).

2.5. Measurements

2.5.1. Tumor growth rates

Each animal was individually tracked for tumor growth by external caliper measurements of protruding tumor. Primary tumor sizes were measured using calipers and an approximate tumor volume calculated using the formula $1/2a \times b^2$, where b is the smaller of two perpendicular diameters.

For each group, the mean and standard error of the mean (S.E.M.) of the ratio V/V_0, relative tumor volume (RTV), were plotted as a function of treatment time after inoculation. V_0 was the tumor volume at Day 0, when treatment began.

2.5.2. Plasma cytokines, and tryptophan and kynurenine levels

Cytokine levels in EDTA plasma from the mice in the first experiment were determined by ELISA assay at Alta Analytical Laboratories (San Diego, CA) using a LINCOplex Kit (Linco Research). Tryptophan (Trp) and kynurenine (Kyn) concentrations were measured from EDTA plasma samples by high pressure liquid chromatography (HPLC) using 3-nitro-L-tyrosine as the internal standard (Widner et al., 1997). To estimate IDO activity, the kynurenine to tryptophan ratio (Kyn/Trp) was calculated and expressed as μmol kynurenine/mmol tryptophan (Wirleitner, 2003). The values from five mice in the first experiment are not included in the summary statistics given in Table 1 for the following reasons. One mouse from each of the four treatment groups was used to test the effects of mega dosing, i.e., with (1:4, mol/mol) calcium pterin at 100 mg/(kg day) after Day 60 of treatment, and are excluded. Also excluded was one mouse from the (1:4, mol/mol) calcium pterin (7 mg/(kg day)) group which expired suddenly a few days before blood was collected. Cytokine measurements <3.2 pg/ml are reported as n.d. (not detectable) because the standard curves used in the ELISA assays were not calibrated below that level.

2.5.3. IDO inhibition determined in vitro with human PBMCs

The purpose of this *in vitro* study was to measure the IC_{50} values of IDO in PBMCs for (1) calcium pterin, $CaCl_2$, and pterin to determine measurable synergistic effects between Ca^{2+} and pterin, and (2) to compare these values with those of DCP for the assessment of relative IDO inhibitory strength. IC_{50} (μM)

values for IDO inhibition by (1:4, mol/mol) calcium pterin, DCP, $CaCl_2$, and pterin were determined *in vitro* with human PBMCs (both PHA-stimulated and unstimulated) by measuring kynurenine production as previously described (Winkler et al., 2006).

2.6. Statistics

Time course statistical analyses based upon repeated measures ANOVA (analysis of variance) models, and standard ANOVA models for group effects, were used (StatView SE + Graphics, v 1.03). Spearman rank order correlations were calculated, and a stepwise regression analysis was carried out (SPSS Graduate Pack 15.0 for Windows, 2006).

3. Results

3.1. Fourier transformed infrared spectrophotometry

Fig. 1 gives the FT-IR spectra of (A) pterin, (B) (1:4, mol/mol) calcium pterin, and (C) DCP (SD045). Relative to pterin, the calcium pterin shows enhanced broad peak signaling at ~3400 cm^{-1} (O–H stretch), consistent with hydration. The calcium pterin spectrum, however, looses the small twin peaks at ~2360 cm^{-1} which are present in the pterin and DCP spectra, since both these latter two compounds have protonizable ring nitrogens (N2 and N3 in Fig. 2B) under the experimental conditions. The twin peaks at ~2360 cm^{-1}, corresponding to these protonated ring nitrogen(s), are not present in the calcium pterin spectrum since calcium complexes with N2 (see Fig. 2A) and sterically blocks N2 (and presumably N3 as well) rendering them unavailable to protonation.

With respect to DCP, we see the following spectral changes relative to pterin: an increased broad peak, with a superimposed sharper peak, in the 3200–3700 cm^{-1} range (O–H and N–H stretches) attributable to hydration and alteration of the aromatic amine electronic environment. A decreased peak, at ~1660 cm^{-1} (C=O stretch) is consistent with calcium complexation of the oxygen. The increased peaks at 1590 and 1540 cm^{-1} (C=N and C=C heterocycle stretches) are unique to DCP. The increased peak at 1460 cm^{-1} (O–H bend) is consistent with the hydration of DCP.

3.2. X-ray crystallographic analysis

The X-ray crystallographic structures of calcium pterin and DCP are given in Fig. 2.

3.3. Antitumor efficacy of calcium pterin

Fig. 3 (first experiment) shows that (1:4, mol/mol) CaPterin at 21 mg/(kg day) significantly inhibits MDA-MB-231 human breast tumor growth in nude mice, giving a 41% *T/C* ratio (mean treatment tumor volume to mean control tumor volume) after 60 days in the first experiment, and 37% *T/C* after 43 days in the second experiment (Fig. 4). The 60-day and 43-day time points represent the longest time periods in each experiment, respectively, during which all the mice survived without confounding reactions. (1:4, mol/mol) CaPterin at 7 mg/(kg day) turned out to be non-significant under the conditions of the first experiment; nevertheless, a dose–response relationship was derived (Fig. 5). Pterin at 21 mg/(kg day) was tested in the first experiment (Fig. 3) as a control and found to have no antitumor activity.

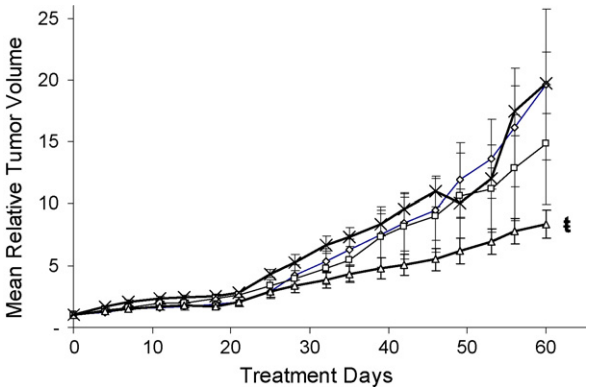

Fig. 3. First experiment: twenty-three athymic nude (nu/nu) female mice, ages 3–4 weeks, were inoculated with 5×10^6 MDA-MB-231 cancer cells subcutaneously into the right flank of each mouse. When tumors reached 3–5 mm in size, twenty of the mice were divided into four treatment groups of five each. Two mice with non-tumor takes were subsequently excluded. Experimental groups were treated by oral gavage once daily with the indicated test suspensions. The control group was treated with sterile water. Overall ANOVA $p = .0175$; $^{\dagger}p < .0001$ vs. control. (◊) (1:4, mol/mol) Calcium Pterin (7 mg/(kg day); $n = 5$); (□) pterin (21 mg/(kg day); $n = 4$); (△) (1:4, mol/mol) calcium pterin (21 mg/(kg day); $n = 5$); (×) control ($n = 4$).

Fig. 4 (second experiment) shows that (1:2, mol/mol) calcium pterin and DCP at both dosages tested, and calcium chloride dihydrate significantly inhibit MDA-MB-231 xenograph growth in nude mice. These efficacy findings identify a new efficacious form of calcium pterin and DCP. Comparison of the control mice

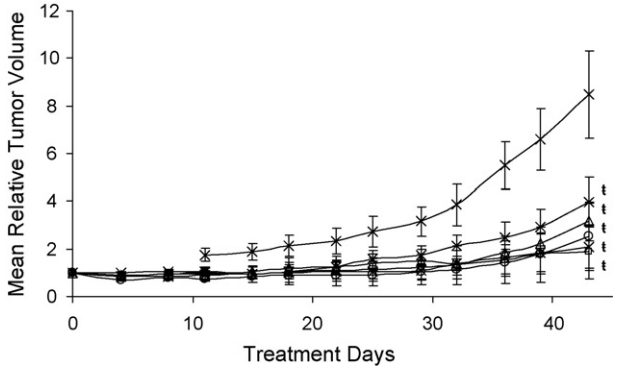

Fig. 4. Second experiment: 29 athymic nude (nu/nu) female mice, ages 3–4 weeks, were inoculated with 10×10^6 MDA-MB-231 cancer cells subcutaneously into the right flank of each mouse. When tumors reached 3–5 mm in size, 25 of the mice were divided into five treatment groups of five mice each. Four mice were assigned as controls. Four mice with non-tumor takes were subsequently excluded. Experimental groups were treated by oral gavage once daily with the indicated test suspensions or solution. The control group was untreated. Overall ANOVA $p < .0001$; $^{\dagger}p < .0001$ vs. control. (△) (1:4, mol/mol) Calcium pterin (21 mg/(kg day), $n = 4$); (□) (1:2, mol/mol) calcium pterin (25 mg/(kg day), $n = 4$); (—✱—) DCP (23 mg/(kg day); $n = 5$); (×) DCP (69 mg/(kg day); $n = 4$); (◯) calcium chloride dihydrate (4.2 mg/(kg day); $n = 5$); (×) control ($n = 3$).

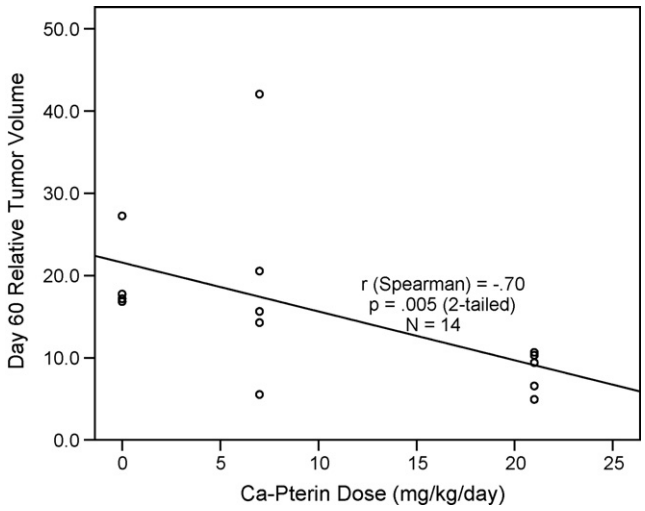

Fig. 5. Dose–response plot of Day 60 relative tumor volume vs. (1:4, mol/mol) calcium pterin (CaPterin) for mice in the first experiment ($n = 14$) with Spearman rank order correlation, $r_s = -.70$; $p = .005$.

tumor growth curves from the first experiment (gavaged with sterile water) and second experiment (untreated) by repeated measures ANOVA found them to be statistically indistinguishable ($p = .99$).

There was no observed toxicity, as determined by body weight changes, among any of the mice in both the first and second experiments. Similarly, there was no observed toxicity (appreciable weight loss) among any of the mice mega-dosed by oral gavage with 100 mg/(kg day) CaPterin for up to 31 days. The greatest weight loss among the mega-dosed group was with one mouse that lost 8.1% (2.1 g) of body weight after 32 days, which included a loss of 400 mm^3 of tumor mass during this period.

3.4. Plasma cytokine levels and IDO activity

Table 1 gives the means and the S.E.M. for the 11 plasma cytokines and IDO measures from the mice in the first experiment, with the exclusions cited in the protocol. ANOVAs determined that none of the cytokine and IDO metabolite plasma concentrations were significantly different across treatment groups by Bonferroni criteria. The large variances for some of the group measures (e.g. IL-12: CaPterin 21 mg/(kg day)) indicate that substantial variability is associated with these plasma levels. Also, no significant rank-order or linear correlations to CaPterin dosage and Day 60 relative tumor volumes by these plasma measures were found. However, multivariate statistical analysis of the data derived, through stepwise regression analysis, a significant underlying pattern of cytokine and IDO metabolite effects attributable to CaPterin dosing (Table 2). For the purposes of this analysis, plasma IL-2 and IL-4 measures were excluded since they were consistently below the limits of detection (<3.2 pg/ml) and other "not detectable" values were set to 3.2 pg/ml, the lowest validated level. The other measures, including IFN-γ, had sufficient variances to be analyzable by the stepwise regression procedure. In the resultant statistically significant ($p < .047$) ACIP (Antitumor Cytokine/IDO Pattern) model, plasma IL-6 and IFN-γ decrease in response to CaPterin dosage, and IL-10 and kynurenine increase. The standard regression coefficients given in Table 2 allow for direct comparison of the relative contributions from each measure in the ACIP model. Table 2 regression was further used to calculate individual ACIP scores for each mouse which are plotted versus Day 60 relative tumor volumes in Fig. 6. Partial regression plots are given in Table 2 for the four ACIP plasma measures of IL-10, IL-6, Kynurenine, and IFN-γ.

3.5. IDO inhibition determined in vitro with human PBMCs

Table 3 gives the IC_{50} values for IDO inhibition determined *in vitro* with human PBMCs, both unstimulated and PHA-stimulated. Normal human calcium and pterin blood levels are also given for comparison. CaPterin and DCP show significantly greater *in vitro* IDO inhibition than either calcium or pterin tested alone in both the unstimulated and PHA-stimulated systems.

4. Discussion

In the current study, (1:4, mol/mol) CaPterin at 7 mg/(kg day) was found not to have significant antitumor activity in the first experiment. In our previous study (Moheno, 2004), (1:4, mol/mol) CaPterin at 7 mg/(kg day) effected a significant 41% *T*/*C* ratio. The difference in efficacies at 7 mg/(kg day) reported in the two studies is attributable to the fact that the MDA-MB-231 tumors grew significantly faster in the Moheno (2004) study, i.e., 9.5-fold in 14 days, versus 2.4-fold in 14 days in the current study (Fig. 3). Faster growing tumors demonstrated a greater percent tumor growth inhibition with CaPterin. The increased tumor growth rate of the MDA-MB-231 cells in the Moheno (2004) study is likely due to the use of a faster growing clone of these cells. Other differences in experimental condition, such as the use of a different stock of nude mice or test article inconsistency, are less likely explanations.

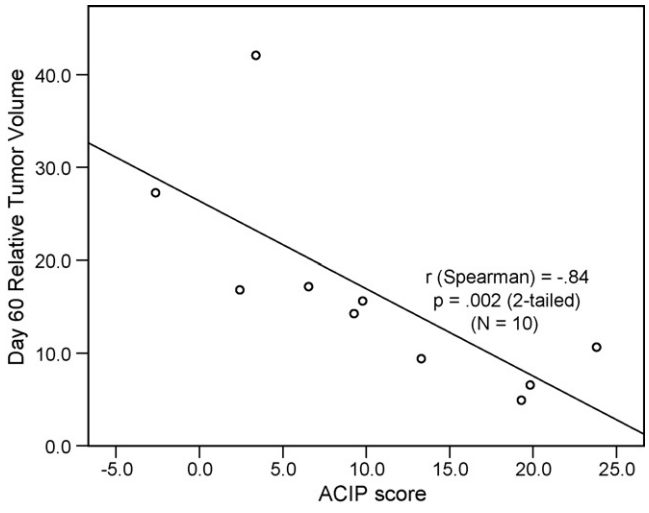

Fig. 6. Day 60 relative tumor volumes plotted vs. ACIP scores (antitumor cytokine/IDO pattern).

Table 2
The antitumor cytokine/IDO pattern (ACIP) induced by CaPterin derived from the stepwise regression of Table 1 data; F-to-enter = 2.0 and F-to-remove = 1.996

	Regression model coefficients*	Standard regression coefficients*
CaPterin dose vs.:	10.5 (intercept)	
Plasma IL-6	−0.096	−0.98
Plasma IL-10	0.31	1.54
Plasma IFN-γ	−3.16	−0.33
Plasma kynurenine	7.89	0.46

The model is significant to *$p = .047$. Standardized partial regression plots are given. ACIP score = 10.5 − 0.096 [IL-6, pg/ml] + 0.31 [IL-10 pg/ml] − 3.16 [IFN-γ pg/ml] + 7.89 [Kyn μM].

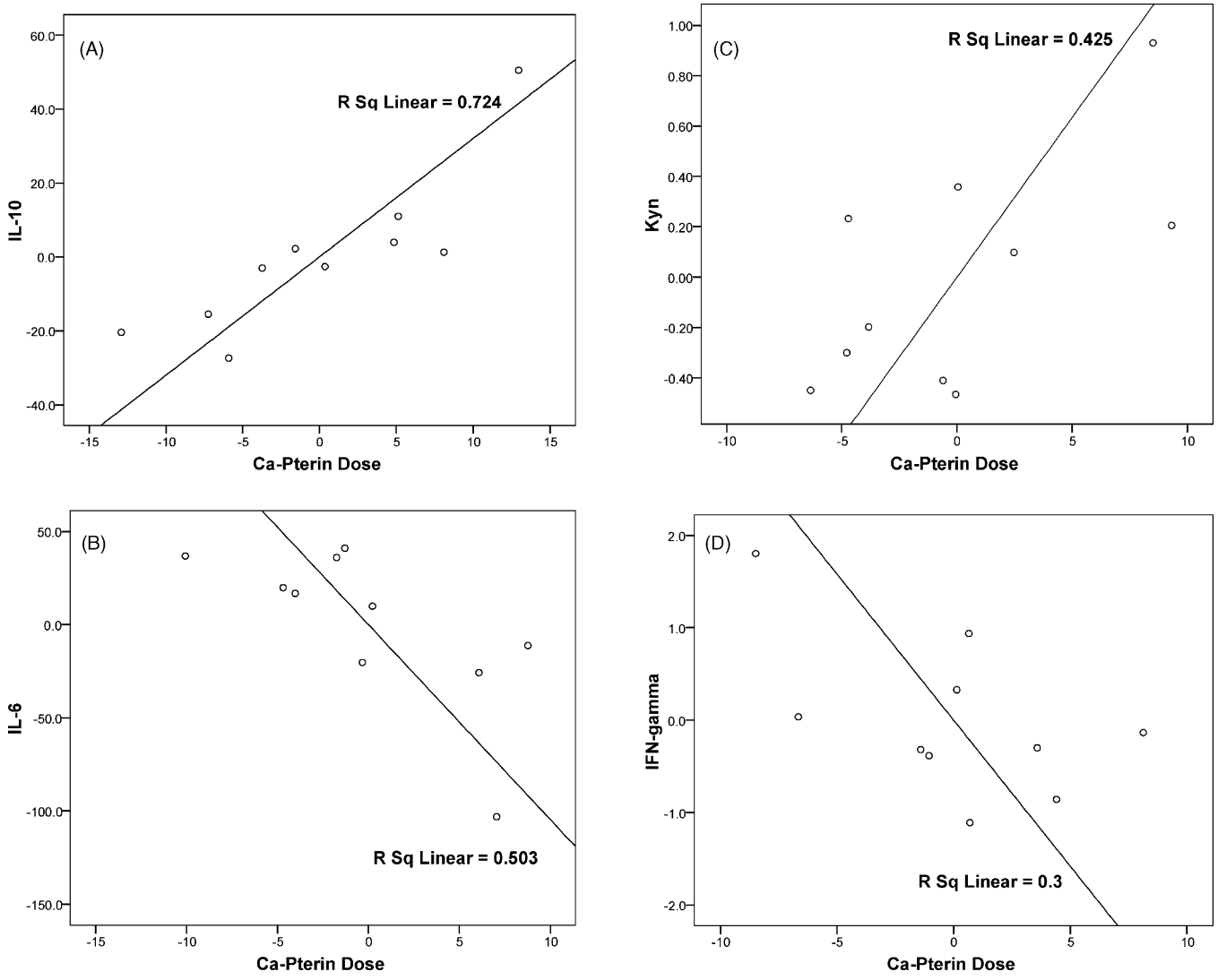

The question as to the role of calcium in mediating the efficacy of the various calcium pterin complexes can be approached by plotting the relative tumor volumes for each treatment group, and the form of the dosed calcium pterin complex, with the dosed calcium equivalent in each complex using the data in the first and second experiments (Fig. 7). Over a six-fold dosing range, from 1 to 6 mg/(kg day) calcium equivalents, comparable antitumor efficacy is apparent among the various calcium forms. The rodent diet given the mice provided an additional 1200 mg/(kg day) of calcium, predominantly in the form of calcium carbonate, and to a much lesser extent calcium pantothenate (230 μg/(kg day) calcium) and calcium iodate (12 μg/(kg day) calcium). Therefore, calcium complexed with pterin, as well as calcium chloride dihydrate, possess antitumor activity not conferred by calcium complexed with carbonate.

Possible explanations for the unexpected tumor growth inhibition observed in the nude mice given calcium chloride dihydrate are that unchelated Ca^{2+} (1) might in some way enhance the antitumor activity of the immune system of the mice, or (2) might have a direct effect upon the MDA-MB-231 breast cancer cells. A third possible explanation is that Ca^{2+}

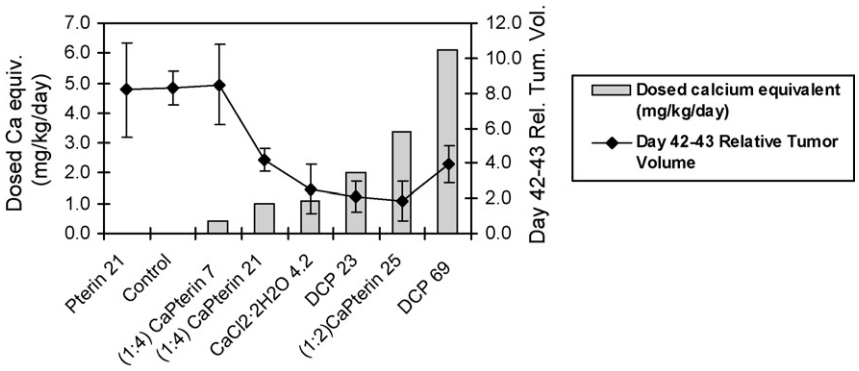

Fig. 7. The calcium equivalent dosed to each group of mice from the first and second experiments is plotted along with the relative tumor volumes recorded at day 42 or 43 of treatment.

ingestion leads to the formation of endogenous calcium pterin in the nude mice. Mice are known to have high liver tetrahydrofolic acid (THF) levels, 6.7 times higher than humans (Johlin et al., 1987). Furthermore, it is known that THF produces pterin upon acid oxidation (Blair and Pearson, 1974). Orally ingested Ca^{2+} ions in the unchelated form (i.e., $CaCl_2$) going from the intestinal tract directly to the liver can lower the pH of the liver and, within the oxidizing tissue environment of the liver, generate pterin from THF which can, in turn, form calcium pterin. This possible explanation can be tested through bioavailability studies measuring mouse plasma pterin changes in response to Ca^{2+} ingestion. Further bioavailability studies can also closely assess the stability of calcium pterin complexes and DCP, and by determining their associated plasma clearance rates and metabolic products, identify bioactive forms.

A significant synergy exists between calcium and pterin in their ability to inhibit IDO in both unstimulated and PHA-stimulated human PBMCs (Table 3). Also, DCP is significantly more active than either $CaCl_2$ or pterin when tested individually. The enhanced IDO inhibition resulting from calcium and pterin synergy in CaPterin is comparable to that found with DCP. Taken together, these *in vitro* studies support the conclusion that calcium-complexed pterin forms (CaPterin and DCP) are more bioactive than their components, calcium and pterin, alone. Comparison of the pterin-equiv as CaPterin IC_{50} values with the pterin levels of normal human blood show that normal blood pterin concentrations are >25,000 times lower, well below estimated therapeutic levels even if fully complexed with calcium. DCP at the highest dose tested in mice in this study, 69 mg/kg, yields the following theoretical body fluid level: $[DCP]_{fluid} = (69\ mg/kg)/(0.7\ L/kg)/(454.4\ mg/mmol) = 220\ \mu M$. This $[DCP]_{fluid}$, estimating a therapeutic mouse body fluid level, is comparable to the *in vitro* IDO IC_{50} values of 470 μM and 320 μM determined for DCP in human PBMCs (Table 3).

Table 3
IC_{50} values for IDO inhibition are given, as determined by kynurenine production *in vitro* for both PHA-stimulated and unstimulated human PBMCs

	Unstimulated IC_{50} (μM)	PHA stimulated IC_{50} (μM)	Normal blood plasma levels
DCP	470	320	
$CaCl_2$	>1400	>1400	~2.3 mM[a]
Pterin	>1200	5300	5–26 nM[b]
Ca-equiv as CaPterin	190	190	
Pterin-equiv as CaPterin	750	750	

Normal human blood levels for calcium and pterin are given for comparison.
[a] Human plasma levels of calcium, which occurs predominantly in several complexed forms.
[b] Human plasma pterin levels as measured in several studies (Andondonskaja-Renz and Zeitler, 1983, 1984; Zeitler et al., 1983; Zeitler and Andondonskaja-Renz, 1987; Eto et al., 1992).

The identified ACIP (antitumor cytokine/IDO pattern) *in vivo* effects of CaPterin dosing, decreased IL-6 and IFN-γ, and increased IL-10 and kynurenine, reveal a pattern of immunological and metabolic responses correlated with CaPterin's antitumor efficacy (Fig. 4 and Table 2), as follows:

(1) An increase in plasma IL-10 correlates with CaPterin dosage. IL-10 has been shown to be a critical, pleiotropic cytokine with contradictory properties (Vicari and Trinchieri, 2004). IL-10 has been mostly observed to possess anti-inflammatory (Th2) properties, antagonizing several functions of antigen-presenting cells (APCs) including dendritic cells (DCs). Investigators have also found ample evidence that IL-10 has a stimulating role in B cell proliferation, as well as natural killer (NK) cell and CD8+ cytotoxic T cell activation. Mocellin et al. (2005) in their review of the available IL-10 evidence conclude that the data appear to support the hypothesis that IL-10 might contribute to the immune-mediated rejection of cancer, at least under some circumstances.
(2) A decrease in plasma IL-6 correlates with increasing CaPterin dosage. The inflammatory cytokine IL-6 is an identified regulator that directs a shift from innate to acquired immunity (Jones, 2005). This immunological switching involves differential control of leukocyte recruitment, activation, and apoptosis. Further study is needed to explain how a down-regulation of IL-6 might regulate this switching in the context of an antitumor response.
(3) A decrease in plasma IFN-γ correlates with increasing CaPterin dosage. The pro-inflammatory cytokine IFN-γ

induces the enzyme IDO in a variety of cells (Wirleitner et al., 2003) which in turn can inhibit the response of T-cells to mitogen stimulation (Schrocksnadel et al., 2006) thus implicating IDO as a tumor escape mechanism (Uyttenhove et al., 2003). The finding that IFN-γ decreases with CaPterin dosages corroborates the findings of (Winkler et al., 2006) that CaPterin inhibits IDO activation in stimulated human PBMCs most likely by decreasing IFN-γ. Strategies to inhibit the IDO pathway may assist in breaking tolerance to tumors, and might enhance the efficacy of immunotherapeutic strategies by removing IDO counter-regulatory inhibition of T-cell activation (Munn, 2006).

(4) The increase in plasma kynurenine correlating with CaPterin dosage can be largely explained by previous findings showing that kynurenine plasma levels correlate with plasma tryptophan levels, both of which decrease with increased tumor load (Schrocksnadel et al., 2006). In those mice dosed with CaPterin, as tumor growth is inhibited, tryptophan and kynurenine plasma levels rise in concert. Since it has been previously shown that *in vitro* (1:4, mol/mol) calcium pterin inhibits IDO in PBMCs as measured by their production of kynurenine (Winkler et al., 2006), it is likely that in the lymphocytic microenvironment IDO is inhibited by calcium pterin, while at the systemic level kynurenine concentrations rise with tumor shrinkage due to the reduced tumor cell demands for circulating tryptophan. The resulting greater concentrations of available plasma tryptophan increase the substrate available to systemic IDO, thereby increasing plasma kynurenine levels as well.

The cytokine plasma changes caused by CaPterin can be generally understood as inducing sustained T-cell activity via IDO inhibition and the modulation of the inflammatory (Th1) immunological system. In addition, CaPterin can also sustain anti-inflammatory (Th2) activity via increased plasma IL-10. Th1 activity, modulated by the inhibition of IDO via decreased IFN-γ, leads to increased T-cell functioning, while Th2 anti-inflammatory activity is sustained by IL-10, which the regression analysis shows is increased by calcium pterin. IL-6, decreased by calcium pterin, reportedly plays a complex switching role between innate and acquired immunities. Significantly, in the context of chronic disease, the blocking of IL-6 signaling is proving to be therapeutically beneficial (Jones, 2005).

In conclusion, our results show that several forms of oral calcium pterin can inhibit MDA-MB-231 xenograph tumors in nude mice. Furthermore, a stepwise regression analysis of plasma cytokine and IDO metabolite levels show four effects correlated with (1:4, mol/mol) calcium pterin dosage: (1) decreased IL-6, (2) increased IL-10, (3) decreased IFN-γ, and (4) increased kynurenine. These findings imply a sustaining effect by calcium pterin of certain inflammatory and anti-inflammatory immunological responses.

The following crystal structure has been deposited at the Cambridge Crystallographic Data Centre and allocated the deposition number CCDC 675775. Ca(pterin)2*5H_2O; C12 H8 Ca1 N10 O7. Unit cell parameters: a 7.097(2), b 16.077(5), c 8.044(3) beta 91.449(4), space group P21/m.

Acknowledgements

The authors would like to express their appreciation for the generous support and assistance from, Dr. Edgar Berkey, Dr. Boris Minev, Dr. Ana María Barral, Dr. Jo Marie Smolec and Jane Ruppel of Alta Analytical Laboratories, Inc., Dr. Richard Scuderi, and the Cancer Federation for these studies.

References

Andondonskaja-Renz, B., Zeitler, H.J., 1983. Separation of pteridines from blood cells and plasma by reverse-phase high-performance liquid chromatography. Anal. Biochem. 133, 68–78.

Andondonskaja-Renz, B., Zeitler, H.J., 1984. Pteridines in plasma and in cells of peripheral blood from tumor patients. In: Pfleiderer, W., Wachter, H., Curtius, H.C. (Eds.), Biochemical and Clinical Aspects of Pteridines: Cancer, Immunology, Metabolic Diseases; Proceedings, Third Winter Workshop on Pteridines, vol. 3, St. Christoph, Arlberg, Austria, Walter de Gruyter & Co., Berlin, New York, February 18–25, 1984, pp. 295–311.

Blair, J.A., Pearson, A.J., 1974. Kinetics and mechanism of the autoxidation of the 2-amino-4-hydroxy-5,6,7,8-tetrahydropteridines. J. Chem. Soc. Perk. II, 80–88.

Eto, I., Bandy, M.D., Butterworth Jr., C.E., 1992. Plasma and urinary levels of biopterin, neopterin, and related pterins and plasma levels of folate in infantile autism. J. Autism Dev. Disord. 22, 295–308.

Johlin, F.C., Fortman, C.S., Nghiem, D.D., Tephly, T.R., 1987. Studies on the role of folic acid and folate-dependent enzymes in human methanol poisoning. Mol. Pharmacol. 31, 557–561.

Jones, S.A., 2005. Directing transition from innate to acquired immunity: defining a role for IL-6. J. Immunol. 175, 3463–3468.

Mocellin, S., Marincola, F.M., Young, H.A., 2005. Interleukin-10 and the immune response against cancer: a counterpoint. J. Leukoc. Biol. 78, 1043–1051.

Moheno, P., 2004. Calcium pterin as an antitumor agent. Int. J. Pharm. 271, 293–300.

Moheno, P., Winkler, C., Fuchs, D., Ryan, J., Meerbergen, E., 2005. Role of calcium pterin in natural killer (NK) cell activation and indoleamine 2,3-dioxygenase (IDO) modulation for antitumor activity. Pteridines 16, 140.

Munn, D.H., 2006. Indoleamine 2,3-dioxygenase, tumor-induced tolerance and counter-regulation. Curr. Opin. Immunol. 18, 220–225.

Schrocksnadel, K., Wirleitner, B., Winkler, C., Fuchs, D., 2006. Monitoring tryptophan metabolism in chronic immune activation. Clin. Chim. Acta 364, 82–90.

Uyttenhove, C., Pilotte, L., Theate, I., Stroobant, V., Colau, D., Parmentier, N., Boon, T., Van den Eynde, B.J., 2003. Evidence for a tumoral immune resistance mechanism based on tryptophan degradation by indoleamine 2,3-dioxygenase. Nat. Med. 9, 1269–1274.

Vicari, A.P., Trinchieri, G., 2004. Interleukin-10 in viral diseases and cancer: exiting the labyrinth? Immunol. Rev. 202, 223–236.

Widner, B., Werner, E.R., Schennach, H., Wachter, H., Fuchs, D., 1997. Simultaneous measurement of serum tryptophan and kynurenine by HPLC. Clin. Chem. 43, 2424–2426.

Winkler, C., Schroecksnadel, K., Moheno, P., Meerbergen, E., Schennach, H., Fuchs, D., 2006. Calcium-pterin suppresses mitogen-induced tryptophan degradation and neopterin production in peripheral blood mononuclear cells. Immunobiology 211, 779–784.

Wirleitner, B., Neurauter, G., Schroecksnadel, K., Frick, B., Fuchs, D., 2003. Interferon-γ-induced conversion of tryptophan: immunologic and neuropsychiatric aspects. Curr. Med. Chem. 10, 1581–1591.

Zeitler, H.J., Andondonskaja-Renz, B., 1987. Evaluation of pteridines in patients with different tumors. Cancer Detect. Prev. 10, 71–79.

Zeitler, H.J., Andondonskaja-Renz, B., Fink, M., Wilmanns, W., 1983. Pteridines in blood cells and plasma: Methods for the quantification of free and conjugated (protein-bound) pteridines. In: Curtius, H.Ch., Pfleiderer, W., Wachter, H. (Eds.), Biochemical and Clinical Aspects of Pteridines: Cancer, Immunology, Metabolic Diseases; Proceedings, Second Winter Workshop on Pteridines, vol. 2, St. Christoph, Arlberg, Austria, Walter de Gruyter & Co., Berlin, New York, March 6–9, 1983, pp. 89–104.